Studies of Spin-Orbit Correlations with Longitudinally Polarized Target

A 12 GeV Research Proposal to Jefferson Lab (PAC 32)

H. Avakian[†*], P.Bosted[†], A. Deur, V.D. Burkert, L.Elouadrhiri
Jefferson Lab, Newport News, VA 23606, USA

K. Griffioen[†]
College of William & Mary, VA 23187, USA

K. Hafidi[†], J. Arrington, L. El Fassi, D. F. Geesaman, R. J. Holt,
D. H. Potterveld, P. E. Reimer, P. Solvignon
Argonne National Lab, Argonne, IL 60439, USA

P. Rossi[†], E. De Sanctis, L. Hovsepyan, M. Mirazita, and S. Anefalos Pereira
INFN, Laboratori Nazionali di Frascati , Via E. Fermi, I-00044 Frascati, Italy

D. Crabb, L.C. Smith
UVA, Charlottesville, VA 22904,USA

M. Amarian, S. Bültmann, S. Kuhn
Old Dominion University, Norfolk, VA 23529, USA

F. Benmokhtar
University of Maryland, USA

Y. Prok
Massachusetts Institute of Technology 77 Massachusetts Avenue Cambridge, MA 02139

D. Ireland, K. Livingston, G. Rosner, B. Seitz
Univ. of Glasgow, Glasgow G12 8QQ, UK

A. Danagoulian, H. Hakobyan
Yerevan State University, 1 Alex Manoogian, Yerevan, Armenia

M. Anselmino, A. Kotzinian, B. Parsamyan, A. Prokudin
Università di Torino and INFN, Sezione di Torino, Via P. Giuria 1, I-10125 Torino
P. Schweitzer, Ruhr-Universitat Bochum, 44780, Bochum Germany
E. Di Salvo, Dipartamento di Fisica and INFN, Sezione di Genova, Via Dodecaneso, 33 I-16146 Genova, Italy
L. Gamberg, Penn State Berks, Reading, PA 19610, USA
G.R. Goldstein, Tufts University, Medford, MA 02155, USA

A CLAS collaboration proposal

[†] Co-spokesperson [*] Contact: Harut Avakian, JLab, Newport News VA 23606. Email: avakian@jlab.org

Collaborators' commitment to the 12 GeV upgrade of Jefferson Lab

- The College of William and Mary group is actively involved in this proposal, as well as several other proposals using CLAS12. Other members of our group are also pursuing a proposal for Hall A, but their contributions are not included here. Among CLAS12 baseline equipment, the group is committed to building part of the forward tracking system, but the exact tasks have not yet been determined. At least one faculty member, two graduate students, half a post-doc and several undergraduates are likely to work at least part time on this project in the next few years. Funding for the group is from the DOE and from the NSF. Additional funding will be sought for building the base equipment. Facilities at William and Mary include a clean room suitable for drift-chamber construction, and, on the time scale of a few years in the future, ample space for detector construction and testing.

- The Laboratori Nazionali di Frascati (LNF) group is actively involved in this proposal. Among CLAS12 equipment, the LNF group plans to contribute to the design, prototyping, construction and testing of the CLAS12 central calorimeter. Three staff members and two post-docs will spend their time as needed on this project. Funding for the group is from the Italian research agency Istituto Nazionale di Fisica Nucleare (INFN). Additional funding are planned to be sought in the European Community.

- Argonne National Laboratory Medium Energy group is actively involved in this proposal, as well as other proposals using CLAS12. Among CLAS12 baseline equipment, the group intends to take responsibility for the design, prototyping, construction and testing of the high threshold Cerenkov counter. 3 research staff and 2 engineers are likely to work at least part time on this project in the next few years. Funding for the group is from DOE. Additional sources of funding will be sought as appropriate. Beyond the baseline equipment, the group is also interested in exploring the possibility of building a RICH detector for CLAS12.

Abstract

We are proposing a comprehensive program to study transverse momentum dependence of valence quark transverse and longitudinal spin distributions through measurements of single-spin and double-spin azimuthal asymmetries in semi-inclusive electroproduction of pions using the upgraded JLab 11 GeV polarized electron beam and the CLAS12 detector with a longitudinally polarized proton and deuteron targets. Main objectives include studies of correlations of the transverse spin of quarks with their transverse momentum, leading to observable single spin asymmetries (SSA), and flavor decomposition of distributions of quarks aligned, q^+, and anti-aligned, q^-, with proton spin as a function of both longitudinal, x, and transverse momentum of the quark, k_T. The measurement of the $\sin 2\phi$ azimuthal moment of the target spin-dependent part of the cross section, in particular will provide direct information on spin-orbit correlations by measuring the leading twist transverse momentum dependent (TMD) parton distribution related to the interference between states with different orbital momenta. The P_T dependence of the double spin asymmetry will provide additional information on the flavor and polarization dependence of transverse momentum dependence of helicity distributions of quarks, providing complimentary to SSA measurements access to spin-orbit correlations. The x, z, P_T and Q^2 dependences of the $\sin\phi$ to $\sin 2\phi$ moments will be studied to probe the underlying T-odd distribution and fragmentation functions as well as verify the hypothesis that the former is twist-3, and the later twist-2. The experiment will use the upgraded CLAS12 detector, 11 GeV highly polarized electron beam, and longitudinally polarized solid ammonia targets (NH_3 and ND_3). Large acceptance of CLAS12, would allow simultaneous detection of the scattered electrons and leading hadrons from the hadronization of the struck quark, providing information on its flavor and transverse momentum. We request 30 days of running on NH_3 and 50 days of running on ND_3 (or possibly ^{6}LiD or HD), including about 20% overhead for target anneals, polarization reversal, and auxiliary measurements.

Contents

1 Introduction

The spin structure of the nucleon has been of particular interest since the EMC [1] measurements implied that the helicity of the constituent quarks account for only a fraction of the nucleon spin. The so-called "spin puzzle" was subsequently confirmed by a number of other experiments at CERN [2], SLAC [3, 4], HERA [5, 6], and JLab [7]. Possible interpretations of this result include the contribution of the orbital momentum of quarks and significant polarization of either the strange sea (negatively polarized) or gluons (positively polarized). The contributions to the sum rule for the total helicity of the nucleon include the following:

$$\frac{1}{2} = \frac{1}{2}\sum_q \Delta q^{val} + \Delta q^{sea} + L_z^{val} + L_z^{sea} + L_z^{glue} + \Delta G, \tag{1}$$

where Δq, L_z, and ΔG are respectively the quark helicity, the orbital angular momentum of all partons, and the gluon helicity.

Present knowledge about the spin structure of the nucleon comes mainly from polarized deep inelastic scattering (DIS). The polarization of the individual flavors and anti-flavors were mainly studied using fits to the inclusive data. Inclusive DIS is sensitive to only the squared charges of the partons, and requires additional assumptions (*e.g.* an SU(3) symmetric sea), which leads to certain ambiguities. Semi-inclusive deep inelastic scattering (SIDIS) studies, when a hadron is detected in coincidence with the scattered lepton that allows so-called "flavor tagging", provide more direct access to contributions from various quarks. In addition, they give access to the transverse momentum distributions of quarks, not accessible in inclusive scattering. Azimuthal distributions of final state particles in semi-inclusive deep inelastic scattering provide access to the orbital motion of quarks and play an important role in the study of transverse momentum distributions of quarks in the nucleon.

Significant progress has been made recently in understanding the role of partonic initial and final state interactions [8, 9, 10]. The interaction between the active parton in the hadron and the spectators leads to gauge-invariant transverse momentum dependent (TMD) parton distributions [8, 9, 10, 11, 12]. Furthermore, QCD factorization for semi-inclusive deep inelastic scattering at low transverse momentum in the current-fragmentation region has been established in Refs. [13, 14]. This new framework provides a rigorous basis to study the TMD parton distributions from SIDIS data using different spin-dependent and independent observables. TMD distributions (see Table 1) describe transitions of a nucleon with one polarization in the initial state to a quark with another polarization in the final state.

The diagonal elements of the table are the momentum, longitudinal and transverse spin distributions of partons, and represent well-known parton distribution functions related to the square of the leading-twist, light-cone wave functions. Off-diagonal elements require non-zero orbital angular momentum and are related to the wave function overlap of L=0 and L=1 Fock states of the nucleon [15]. The parton distributions $f_{1T}^{\perp}$ and $h_1^{\perp}$ represent the imaginary parts of the corresponding interference terms, while the functions g_{1T} and $h_{1L}^{\perp}$ represent their real parts. The TMDs $f_{1T}^{\perp}$ (chiral-even) and $h_1^{\perp}$ (chiral-odd) are known as the Sivers and Boer-Mulders functions [16, 17, 18, 9, 10, 11]. They describe unpolarized quarks in the transversely polarized nucleon and transversely polarized quarks in the unpolarized nucleon respectively. They vanish at tree-level in a T-reversal invariant model (T-odd) and can only be non-zero when initial or final state interactions cause an interference between

N/q	U	L	T
U	$\mathbf{f_1}$		$h_1^\perp$
L		$\mathbf{g_1}$	$h_{1L}^\perp$
T	$f_{1T}^\perp$	g_{1T}	$\mathbf{h_1}$ $h_{1T}^\perp$

Table 1: Leading-twist transverse momentum-dependent distribution functions. U, L, and T stand for transitions of unpolarized, longitudinally polarized, and transversely polarized nucleons (rows) to corresponding quarks (columns).

different helicity states. These functions parametrize the correlation between the transverse momentum of quarks and the spin of a transversely polarized target or the transverse spin of the quark, respectively. They require both orbital angular momentum, as well as non-trivial phases from the final state interaction, that survive in the Bjorken limit. Experimental results on the Sivers functions for up and down quarks so far are consistent with a heuristic model of up and down quarks orbiting the nucleon in opposite directions. The most simple mechanism that can lead to a Boer-Mulders function is a correlation between the spin of the quarks and their orbital angular momentum. The T-even counterpart of the Boer-Mulders function, $h_{1L}^\perp$, which is one of the main focuses of the current proposal describes the correlations of the transverse spin of quarks in the longitudinally polarized nucleon and their transverse momentum.

The off-diagonal TMD distributions arise from interference between amplitudes with left- and right-handed polarization states, and only exist because of chiral symmetry breaking in the nucleon wave function in QCD. Their study therefore provides a new avenue for probing the chiral nature of the partonic structure of hadrons. The universality of the TMD correlation functions has been proven, resulting in a sign change for two T-odd TMD distributions between Drell-Yan and DIS [9, 14], an exciting prediction that has to be confirmed by future experiments.

Similar correlations arise in the hadronization process. One particular case is the Collins T-odd fragmentation function $H_1^\perp$ [19] describing fragmentation of transversely polarized quarks into unpolarized hadrons. Parton model analyses [20, 21, 22, 23] of sub-leading single-spin asymmetries observed at HERMES [24, 25] and CLAS [26] lead to the introduction of new twist-3 T-odd distribution functions [14, 12].

In recent years, semi-inclusive deep inelastic scattering (SIDIS) has emerged as a powerful tool to probe nucleon structure through transverse single spin asymmetries (SSAs) [24, 27, 28]. In contrast to inclusive deep inelastic lepton-nucleon scattering where transverse momentum is integrated out, these processes are sensitive to transverse momentum scales on the order of the intrinsic quark momentum $P_T \sim k_\perp$.

Orbital momentum of quarks changes significantly the helicity distribution of quarks in the valence quark region, in particular the distributions of quarks anti-aligned, with proton spin [29]. Simple model calculations also indicate that quark distributions aligned, q^+, and anti-aligned, q^-, with proton spin will have also very different transverse momentum distributions [30]. That may lead to observable effects in transverse momentum, P_T, dependences of double-spin longitudinal asymmetries [31]. Correlations of transverse spin of quarks in

the longitudinally polarized nucleons and their transverse momentum also lead to observable Single Spin Asymmetries (SSAs)[32].

The JLab 12-GeV upgrade will provide the unique combination of wide kinematic coverage, high beam intensity (luminosity), high energy, high polarization, and advanced detection capabilities necessary to study the transverse momentum and spin correlations in double-polarized semi-inclusive processes both in the target and current fragmentation regions.

1.1 Spin and Azimuthal Asymmetries in SIDIS

The SIDIS cross section at leading twist has eight contributions related to different combinations of the polarization state of the incoming lepton and the target nucleon [33, 13].

$$\begin{aligned}\frac{d\sigma}{dxdydz_h d^2\vec{P}_{h\perp}} &= \tfrac{4\pi\alpha_{\rm em}^2 s}{Q^4}(1-y+y^2/2)xF_{UU}^{(1)} - (1-y)x\cos(2\phi_h)F_{UU}^{(2)} \\ &+\lambda S_L y(1-y/2)xF_{LL} + S_L(1-y)x\sin(2\phi_h)F_{UL} \\ &+|S_T|(1-y+y^2/2)x\sin(\phi_h-\phi_S)F_{UT}^{(1)} \\ &+|S_T|(1-y)x\sin(\phi_h+\phi_S)F_{UT}^{(2)} \\ &+\lambda|S_T|y(1-y/2)x\cos(\phi_h-\phi_S)F_{LT} \\ &+\tfrac{1}{2}|S_T|(1-y)x\sin(3\phi_h-\phi_S)F_{UT}^{(3)}] \end{aligned} \quad (2)$$

The kinematic variables x, y are defined as: $x = Q^2/2(P_1q)$, and $y = (P_1q)/(P_1k_1)$. The variable $q = k_1 - k_2$ is the momentum of the virtual photon, $Q^2 = -q^2$, ϕ_h is the azimuthal angle between the scattering plane formed by the initial and final momenta of the electron and the production plane formed by the transverse momentum of the observed hadron and the virtual photon (see Fig. 1), ϕ_S is the azimuthal angle of the transverse spin in the scattering plane. The subscripts in F_{UL}, F_{LL},etc., specify the beam (first index) and target(second index) polarizations, longitudinal (L), transverse (T), unpolarized (U),

Structure functions factorize into TMD parton distributions and fragmentation functions, and into soft and hard parts [13]

$$\begin{aligned}\sigma_{UU} \propto F_{UU} \propto &\quad f_1(x,k_\perp)\, D_1(z_h,p_\perp)\, S(\vec{\ell}_\perp) H_{UU}(Q^2) \\ \sigma_{LL} \propto F_{LL} \propto &\quad g_{1L}(x,k_\perp)\, D_1(z_h,p_\perp)\, S(\vec{\ell}_\perp) H_{LL}(Q^2) \\ \sigma_{UL} \propto F_{UL} \propto &\quad h_{1L}^\perp(x,k_\perp)\, H_1^\perp(z_h,p_\perp)\, S(\vec{\ell}_\perp) H_{UL}(Q^2), \end{aligned} \quad (3)$$

where $z = (P_1P_h)/(P_1q)$, $k_\perp$ and $p_\perp$ are quark transverse momenta before and after scattering, and P_1 and P_h are the four momenta of the initial nucleon and the observed final-state hadron respectively.

The unpolarized D_1 and polarized $H_1^\perp$ fragmentation functions depend in general on the transverse momentum of the fragmenting quark.

S_L and S_T are longitudinal and transverse components of the target polarization with respect to the direction of the virtual photon. The different hard factors (H_{UU}, H_{LL},etc.), which are calculable in pQCD, in the SIDIS cross section are similar at one-loop order [13]

and may cancel to a large extent in asymmetry observables. The soft factor $S(\vec{\ell}_\perp)$ comes from soft gluon radiation and is defined by a matrix element of Wilson lines in the QCD vacuum [13]. With a certain choice of factorization parameters, the soft factor could become unity. This may explain the success of existing phenomenology, based on the "naive" factorization assumption [34].

In the case of the polarized beam and target the cross section has contributions that depend on the spin of the target or the spin of the beam or both and involve all 8 leading twist TMD distribution functions [34, 35, 36, 22].

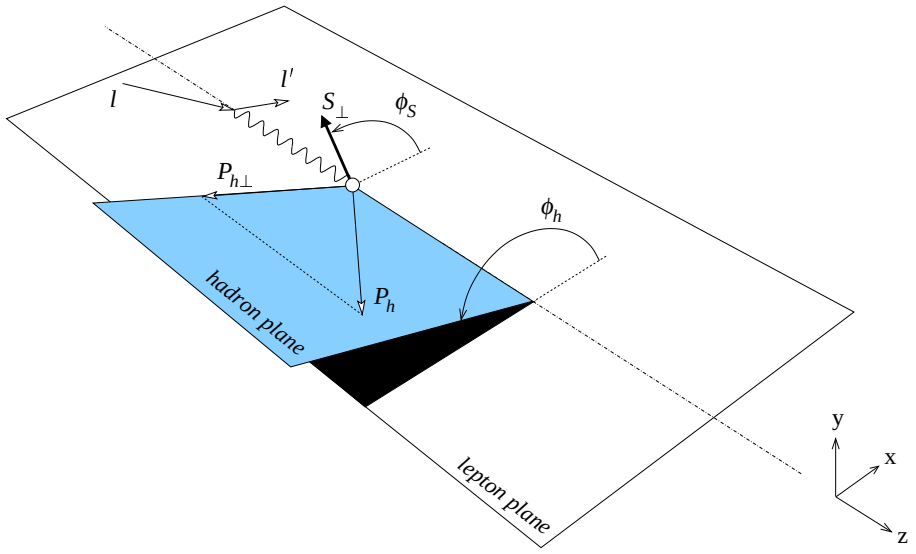

Figure 1: SIDIS kinematics. For a longitudinally polarized target, ϕ_S=0 or 180^o for negative and positive helicities of the proton, respectively.

During the last few years, first results on transverse SSAs have become available [27, 28]. Pioneering measurements by HERMES Collaboration for the first time directly indicated significant azimuthal moments generated both by Collins ($F_{UT}^{(2)}$) and Sivers ($F_{UT}^{(1)}$) effects.

1.1.1 Spin-Azimuthal Asymmetries in SIDIS

Spin-orbit correlations are accessible in SIDIS with longitudinally polarized target in measurements of double and single-spin asymmetries. For a longitudinally polarized target the only azimuthal asymmetry arising in leading order is the $\sin 2\phi$ moment,

$$\sigma_{UL}^{\sin 2\phi} \propto S_L 2(1-y) \sin 2\phi \sum_{q,\bar{q}} e_q^2 x h_{1L}^{\perp q}(x) H_1^{\perp q}(z). \tag{4}$$

The distribution function giving rise to SSA, $h_{1L}^\perp$, is related to the real part of the interference of wave functions for different orbital momentum states, and describes transversely polarized quarks in the longitudinally polarized nucleon. The physics of σ_{UL}, which involves the Collins fragmentation function $H_1^\perp$ and Mulders distribution function $h_{1L}^\perp$, was first discussed by Kotzinian and Mulders in 1996 [34, 33, 32]. The same distribution function is accessible in double polarized Drell-Yan, where it gives rise to the $\cos 2\phi$ azimuthal moment

in the cross section [37]. The behavior of the Mulders distribution function was recently studied both in large-x [38] and large N_c [39] limits of QCD.

Measurements of the $\sin 2\phi$ SSA [32], allows the study of the Collins effect with no contamination from other mechanisms. A recent measurement of the $\sin 2\phi$ moment of σ_{UL} by HERMES [24] is consistent with zero. A measurably large asymmetry has been predicted only at large x ($x > 0.2$), a region well-covered by JLab [20].

The measurement of transverse spin dependent distributions is complicated by the presence of an essentially unknown Collins function. Calculations of the Collins function for pions in a chiral invariant approach at a low scale [40] indicate that at large z the function rises much faster than previously predicted [20, 41] in the analysis using the HERMES data on target SSA. It was also pointed out that the ratio of polarized and unpolarized fragmentation is almost scale independent [40]. Recently a significant asymmetry was measured by Belle [42] in e^+e^- annihilation to pions, indicating that the Collins function is indeed large. The transverse asymmetry measurements involving the transverse spin distributions in a transversely polarized nucleon and Collins fragmentation function, were performed at HERMES [43] and COMPASS [28].

Assuming that the transverse spin of the sea quarks in longitudinally polarized nucleon is negligible ($h_{1L}^{\perp\bar{q}} = 0$) and ignoring the non-valence quark contributions in π^+ production and unfavored fragmentation, the single-spin transverse asymmetry arising from fragmentation becomes:

$$A_{UL}^{\pi^+} \propto \frac{4h_{1L}^{\perp(1)u}(x)}{4u(x) + \bar{d}(x)} \frac{H_1^{\perp u\to\pi^+}(z, P_\perp)}{D_1^{u\to\pi^+}(z, P_\perp)}, \tag{5}$$

where $h_{1L}^{\perp(1)}$ means integration over the transverse momentum weighted with k_T^2. Similar formulas available for neutron target replacing u and d and also for π^- and π^0. For them, however, the contribution from unfavored fragmentation will be significant and should be accounted in the extraction. Measurements of transverse momenta of final state hadrons in SIDIS with longitudinally polarized targets will thus provide complementary to transverse target information, probing the longitudinal nucleon structure beyond the collinear approximation.

Based on the leading order, similar procedure has been applied recently [44] to extract the transversity distribution, combining e^+e^- and semi-inclusive DIS data [27]. The statistics, however, are not enough to make statistically significant predictions in the valence region, where the effects are expected to be large.

Measurements of transverse momentum dependence of helicity distributions will be also important for interpretation of ongoing studies at different facilities worldwide of gluon polarization using high P_T hadrons [45, 46, 47, 48].

1.2 Flavor and transverse momentum dependence of helicity distributions

Deviations of existing data from pQCD based parameterizations at large-x are more significant for distributions of quarks anti-aligned ($u^-(x), d^-(x)$) with proton spin (see Fig. 2) which are expected to be more sensitive to contributions from the orbital motion of quarks

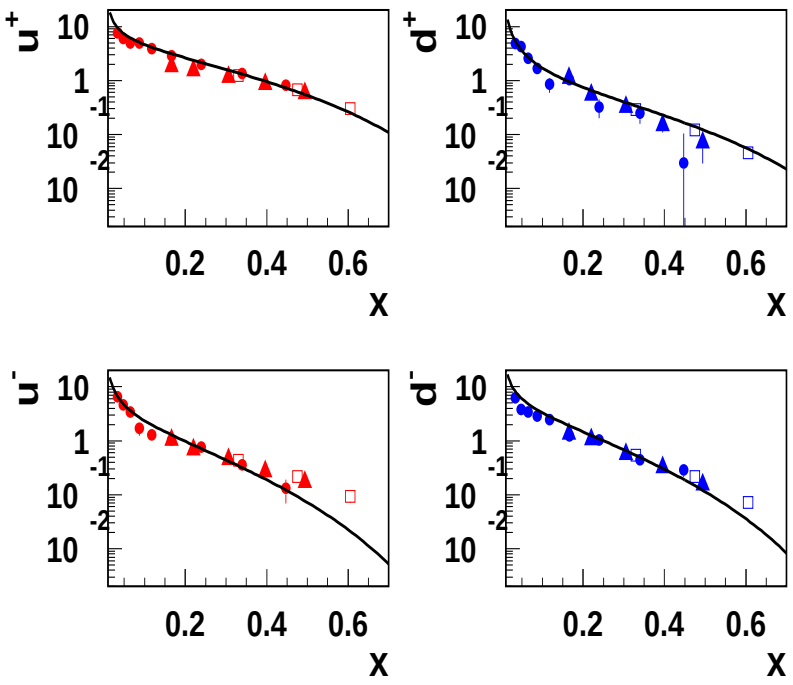

Figure 2: Helicity distributions compared to LSS parametrization [49]. Circles,triangles and open squares represent HERMES, CLAS and Hall-A data respectively.

[29]. Simple model calculations indicate that the distribution of quarks anti-aligned with proton spin will have much wider in transverse momentum distributions compared to quarks with spins aligned with proton spin $(u^+(x), d^+(x))$.

Differences in the transverse momentum dependent distributions for different helicity states leads to observable effects in double spin asymmetry measurements as a function of P_T of the hadron [31]. Assuming a simple Gaussian dependence the corresponding TMD distributions are given by:

$$f_1^q(x,k_\perp) = f_+^q(x)\frac{1}{\pi\mu_+^2}\exp\Big(-\frac{k_\perp^2}{\mu_+^2}\Big) + f_-^q(x)\frac{1}{\pi\mu_-^2}\exp\Big(-\frac{k_\perp^2}{\mu_-^2}\Big) \quad (6)$$

$$g_{1L}^q(x,k_\perp) = f_+^q(x)\frac{1}{\pi\mu_+^2}\exp\Big(-\frac{k_\perp^2}{\mu_+^2}\Big) - f_-^q(x)\frac{1}{\pi\mu_-^2}\exp\Big(-\frac{k_\perp^2}{\mu_-^2}\Big)\ , \quad (7)$$

where $f_1^q(x)$, $g_{1L}^q(x)$, $f_+^q(x)$, and $f_-^q(x)$ are related by:

$$f_1^q(x) = f_+^q(x) + f_-^q(x) \quad (8)$$

$$g_{1L}^q(x) = f_+^q(x) - f_-^q(x)\ . \quad (9)$$

Corresponding cross sections are given by:

$$\Delta\sigma_{LL} = \frac{y(2-y)}{xy^2}\frac{1}{\mu_D^2+z\mu_+^2}\exp\Big(-\frac{P_{hT}^2}{\mu_D^2+z\mu_+^2}\Big)\,\Sigma_q e_q^2 f_+^q(x)D_q^h(z) \quad (10)$$
$$- \frac{y(2-y)}{xy^2}\frac{1}{\mu_D^2+z\mu_-^2}\exp\Big(-\frac{P_{hT}^2}{\mu_D^2+z\mu_-^2}\Big)\,\Sigma_q e_q^2 f_-^q(x)D_q^h(z)$$
$$\sigma_0 = \frac{1+(1-y)^2}{xy^2}\frac{1}{\mu_D^2+z\mu_+^2}\exp\Big(-\frac{P_{hT}^2}{\mu_D^2+z\mu_+^2}\Big)\,\Sigma_q e_q^2 f_+^q(x)D_q^h(z) \quad (11)$$
$$+ \frac{1+(1-y)^2}{xy^2}\frac{1}{\mu_D^2+z\mu_-^2}\exp\Big(-\frac{P_{hT}^2}{\mu_D^2+z\mu_-^2}\Big)\,\Sigma_q e_q^2 f_-^q(x)D_q^h(z)\ .$$

Detailed measurements of A_{LL} and its $\cos\phi$ moment as a function of P_T in different bins in x, z, Q^2 combined with measurements of azimuthal moments of the unpolarized cross section proposed for `CLAS12` will allow study of the flavor dependence of transverse momentum distributions. The $P_\perp$-dependence of the double-spin asymmetry, measured for different bins in z and x will also provide a test of the factorization hypothesis and probe the transition from the non-perturbative to perturbative description. At large P_T ($\Lambda_{QCD} << P_T << Q$) the asymmetry is expected to be independent of $P_\perp$ [13]. In the first approximation the parameters $\mu^\pm$ could be extracted from fits to measured double-spin asymmetries for different final state pions.

Flavor decomposition of transverse momentum dependent valence helicity distributions $u^+(x,k_T), u^-(x,k_T), d^+(x,k_T), d^-(x,k_T)$ will require good knowledge of unpolarized distributions of hadrons in the same bins and also an upgrade of both standard flavor decomposition procedures described below.

First method makes use of particular combinations of measurements that will directly yield information on the underlying quark polarizations (at least in leading order), without requiring knowledge of fragmentation functions.

One such quantity is the SIDIS pion asymmetry [50]

$$A^{\pi^+-\pi^-} = \frac{N_{\uparrow\downarrow}^{\pi+} - N_{\uparrow\downarrow}^{\pi-} - N_{\uparrow\uparrow}^{\pi+} + N_{\uparrow\uparrow}^{\pi-}}{N_{\uparrow\downarrow}^{\pi+} - N_{\uparrow\downarrow}^{\pi-} + N_{\uparrow\uparrow}^{\pi+} - N_{\uparrow\uparrow}^{\pi-}}. \quad (12)$$

This asymmetry can be measured on the proton and the deuteron and only depends on the valence quark distributions u_V, Δu_V, d_V and Δd_V:

$$A_p^{\pi^+-\pi^-}(x) = \frac{4\Delta u_V(x) - \Delta d_V(x)}{4u_V(x) - d_V(x)} \qquad A_d^{\pi^+-\pi^-}(x) = \frac{\Delta u_V(x) + \Delta d_V(x)}{u_V(x) + d_V(x)}, \quad (13)$$

at least in a kinematic region where one is not completely dominated by sea quarks. It should be noted that the fragmentation functions cancel in the definition of the asymmetry above. Using the above system of equations and measurements of the unpolarized distribution functions $u_V(x)$ and $d_V(x)$, one can extract the polarized valence quark distribution functions $\Delta u_V(x)$ and $\Delta d_V(x)$ from SIDIS asymmetry measurements.

SMC measured DIS and SIDIS asymmetries using polarized muons as the probe and polarized ammonia or deuterated butanol as the proton and deuteron target, respectively.

They extracted Δq (in LO) using a system of equations involving both the DIS and SIDIS measurements.

The HERMES Collaboration has extracted LO polarized quark distribution functions from SIDIS measurements [6] using a similar method commonly referred to as the "Purity" method (basically an extension of the SMC approach above). The Purity $\mathcal{P}_q^h(x, Q^2, z)$ represents the probability that the observed final state hadron h originated from a quark of flavor q and is defined in terms of the unpolarized quark distributions such that

$$\mathcal{P}_q^h(x, Q^2, z) = \frac{e_q^2 q(x, Q^2) D_q^h(z, Q^2)}{\sum_{q'} e_{q'}^2 q'(x, Q^2) D_{q'}^h(z, Q^2)}. \tag{14}$$

The assumption that the hard scattering process and fragmentation may be factorized leads to

$$A_1^h(x, Q^2, z) = \sum_q \mathcal{P}_q^h(x, Q^2, z) \frac{\Delta q(x, Q^2)}{q(x, Q^2)} \tag{15}$$

A fitting procedure is again implemented which uses minimization methods to solve the vector equation equivalent of Eq. 15 :

$$\vec{A} = \mathcal{P}\vec{Q} \tag{16}$$

where $\vec{A}$ contains both inclusive and semi-inclusive asymmetry measurements on both proton and deuteron targets and $\vec{Q}$ represent the ratio of polarized to unpolarized quark distribution functions. The Purity method relies on the LUND model's [51] ability to describe the quark fragmentation process. In practice, the HERMES collaboration determines $\mathcal{P}$ using a LUND based Monte Carlo simulation tuned to reproduce the hadron multiplicities observed by the HERMES experiment.

To perform a P_T-dependent flavor decomposition double spin asymmetries have to be extracted in bins in P_T. The P_T-dependent cross section is given by[31]:

$$\sigma_{LL} = \frac{\pi}{xy^2} \left[\, y(2-y) \, \right] \Sigma_q e_q^2 \int d^2\mathbf{k}_\perp \; g_{1L}^q(x, \mathbf{k}_\perp) \; D_q^h(z, \mathbf{P}_{hT} - z\mathbf{k}_\perp) \; , \tag{17}$$

$$\sigma_0 = \frac{\pi}{xy^2} \left[\, 1 + (1-y)^2 \, \right] \Sigma_q e_q^2 \int d^2\mathbf{k}_\perp \; f_1^q(x, \mathbf{k}_\perp) \; D_q^h(z, \mathbf{P}_{hT} - z\mathbf{k}_\perp) \; . \tag{18}$$

Measured single and double spin asymmetries for all pions in a large range of kinematic variables (x_B, Q^2, z, $P_\perp$, and ϕ) combined with measurements with unpolarized targets will provide detailed information on the flavor and polarization dependence of the transverse momentum distributions of quarks in the valence region, and in particular, on the x_B, z, and $P_\perp$ dependence of the leading TMD parton distribution functions of u and d quarks. Such measurements across a wide range of x, Q^2, and P_T would allow for detailed tests of QCD dynamics in the valence region complementing the information obtained from inclusive DIS. They would also serve as novel tools for exploring nuclear structure in terms of the quark and gluon degrees of freedom of QCD.

1.3 Data on SSA and Helicity Structure

The preliminary data from CLAS at 6 GeV indeed indicate large azimuthal moments both for $\sin\phi$ and $\sin 2\phi$ (Fig.4). The data on kinematic dependence of the leading-twist SSA are shown in Fig. 3. Calculations were done using $h_{1L}^{\perp}$ from the chiral quark soliton model evolved to Q^2=1.5 GeV^2 [20], f_1 from GRV95 [52], and D_1 from Kretzer, Leader, and Christova [53]. The curves correspond to dominance of the favored fragmentation $H_1^{\perp u\to\pi^+}$. An important ingredient for the estimates are so-called "Lorentz-invariance relations" that connect $h_{1L}^{\perp}$ with h_1 [34]. Meanwhile these relations are known not to be valid exactly [54, 55]. It is of importance to find out experimentally to which extent such relations can provide useful approximations, or whether they are badly violated, since there is little theoretical intuition on that point.

The kinematic dependence of the SSA for π^+, measured from the CLAS EG1 data set at 6 GeV is consistent with predictions [20]. The π^+ SSA is dominated by the u-quarks; therefore with some assumption about the ratio of unfavored to favored Collins fragmentation functions, it can provide a first glimpse of the twist-2 Mulders TMD function. The distribution function $h_{1L}^{\perp}$ was extracted using the π^+ target SSA [56], which is less sensitive to the unknown ratio of unfavored (d-quark fragmenting to π^+) to favored (u-quark fragmenting to π^+) polarized fragmentation functions (see Fig. 9). The curve is the result of the calculation by Efremov et al. [20], using $h_{1L}^{\perp}$ from the chiral quark soliton model evolved to Q^2=1.5 GeV^2. The extraction, however, suffers from low statistics and has a significant systematic error from the unknown ratio of the Collins favored and unfavored fragmentation functions, the unknown ratio of h_{1L}^d/h_{1L}^u, as well as from background from exclusive vector mesons. Current statistical errors for π^-, and in particular π^0, which is relatively free of possible higher twist contributions [57], are large and do not allow strong conclusions from the measured SSAs. More data are required for a statistically significant measurement of the $\sin 2\phi$ moment.

Measurements of transverse momenta of final state hadrons in SIDIS with longitudinally polarized targets will provide complementary to transverse target information, probing the longitudinal nucleon structure beyond the collinear approximation. The $P_\perp$-dependence of the double-spin asymmetry, measured for different bins in z and x will provide a test of the factorization hypothesis and probe the transition from the non-perturbative to perturbative description. At large P_T ($\Lambda_{QCD} << P_T << Q$) the asymmetry is expected to be independent of $P_\perp$ [13].

There are indications that the double-spin asymmetry (see Fig. 10) at small P_T tends to increase for π^- and decrease for π^+. A possible interpretation of the P_T-dependence of the double spin asymmetry may involve different widths of transverse momentum distributions of quarks with different flavor and polarization [31] resulting from a different orbital structure of quarks polarized in the direction of the proton spin and opposite to it [58, 59]. This interpretation may demand a different width for d-quarks than for u-quarks, consistent with observation from lattice QCD studies of a different spread in transverse distances for d-quarks compared to u-quarks [60]. The same effect may be responsible for the relatively large $\cos\phi$ moment of the double spin asymmetry (see Fig.10, right panel).

Detailed measurements of A_{LL} and its $\cos\phi$ moment as a function of P_T in different bins in x, z, Q^2 combined with measurements of azimuthal moments of the unpolarized cross section

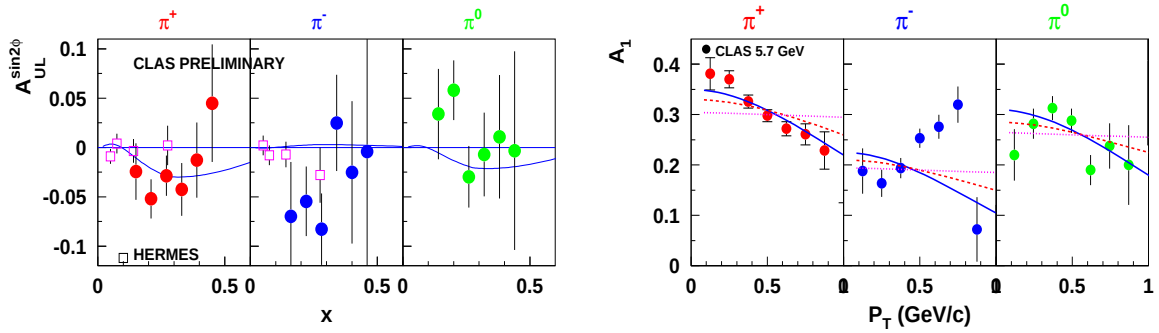

(a) (b)

Figure 3: Measurements of single (left) and double (right) spin asymmetries as a function of x and P_T. The open squares show the HERMES data, and filled symbols are for CLAS preliminary results at 5.7 GeV. The curves are calculated using Ref. [61] and [31] (right).

proposed for CLAS12 will allow study of the flavor dependence of transverse momentum distributions.

SIDIS experiments exploit the statistical correlation between the flavor of the struck quark and the type of hadron produced to extract information on quark and antiquark PDFs of all flavors separately. The SMC experiment at CERN [62] measured DIS and SIDIS asymmetries using polarized muons as the probe and polarized ammonia or deuterated butanol as the proton and deuteron target, respectively. This experiment has been followed by the COMPASS experiment at CERN [28] which is now collecting data. The HERMES collaboration at DESY [6] uses polarized electron and positron beams stored in the HERA electron proton collider and an internal polarized gas target. The present data set in the intermediate range of x ($0.1 \leq x \leq 0.3$) is mainly coming from HERMES (see Fig.5) and has relatively large uncertainties. Additional data from SIDIS using CLAS12 will allow a precision fit to $\frac{\Delta u}{u}$ and $\frac{\Delta d}{d}$ to extract valence quark distributions and study the contributions from Orbital Angular Momentum (OAM).

Our present knowledge of polarized sea quark distributions from these experiment is also rather limited. HERMES results on Δs are consistent with zero for the x-region covered, while DIS data seem to indicate a negative contribution of the strange sea to the nucleon spin.

The goal of our proposed experiment is to gather a vastly larger data set on SIDIS in the region $0.1 \leq x \leq 0.8$, $0 \leq P_T \leq 1.2$, and $0.2 \leq z \leq 0.8$. Global analysis of the data will provide fits to transverse momentum dependent helicity distributions and allow extraction of contribution of OAM to distributions over the longitudinal momentum. With the present configuration of CLAS12, kaons can only be separated from pions below a momentum of 4.5 GeV/c and will yield only limited additional constraints, especially on the strange and non-strange sea.

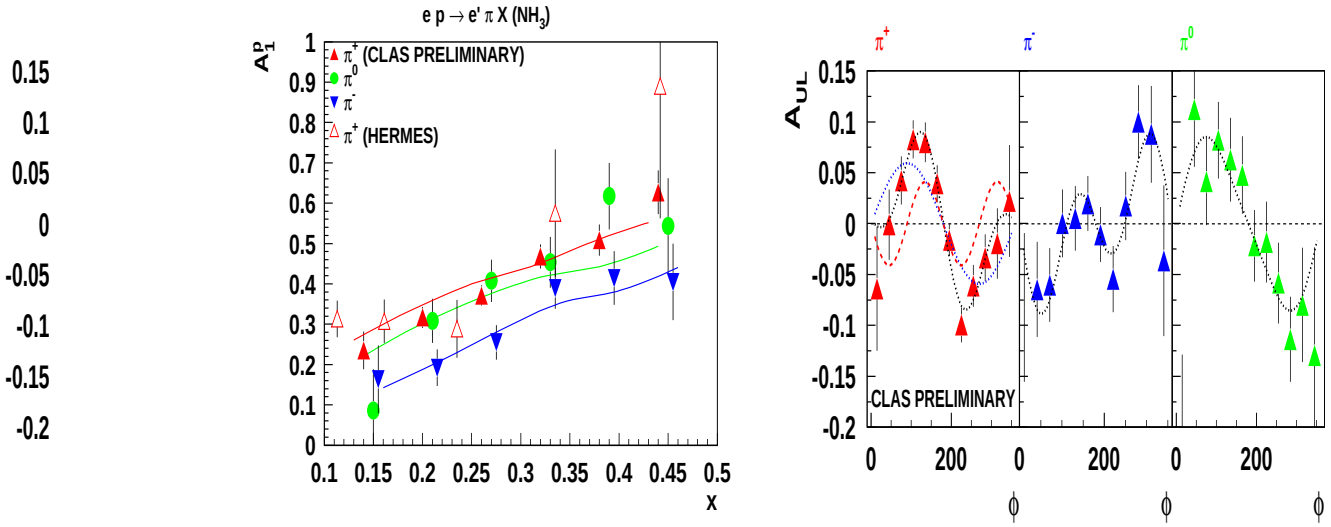

(a) (b)

Figure 4: Comparison of various SIDIS asymmetries measured with 5.7 GeV beam in CLAS with predictions from hadronization models and higher energy data. Right Panel shows preliminary SSAs results from CLAS at 5.7 GeV with fits.

2 Experimental Details

2.1 CLAS12

The proposed experiment will use the upgraded CLAS12 spectrometer in its standard configuration. We will run at the maximum magnetic field. Running conditions will be similar to already approved CLAS12 proposal for inclusive DIS studies with CLAS12 [63]. The central tracker will also be used for coincident detection of protons and pions. The solenoid for the central tracker is also used simultaneously to provide the magnetic field for the polarized target. Additional details on CLAS12 can be found in the document provided as an appendix to all CLAS12 proposals.

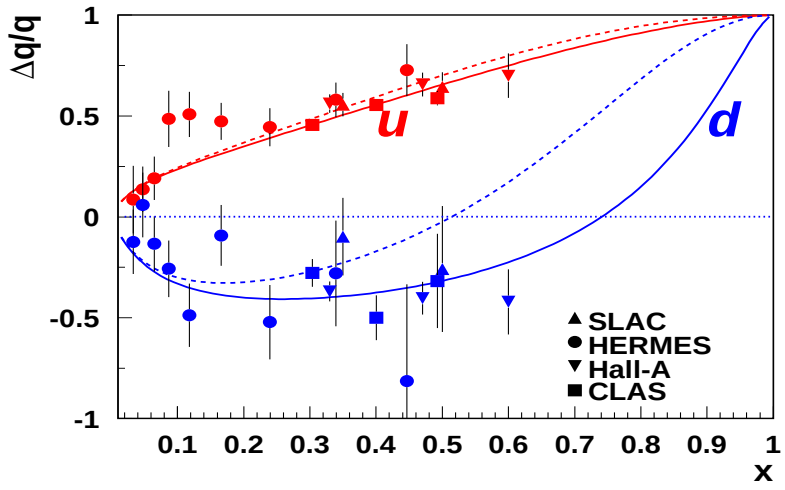

Figure 5: Helicity distributions from the SLAC, Hermes and CLAS experiments compared to pQCD based predictions with (solid line) and without (dashed line) orbital angular momentum.

2.2 Polarized Target

The proposed experiment requires use of a polarized solid state target. The target will be polarized via the method of Dynamic Nuclear Polarization (DNP) which is a well established technique that has been used extensively in nuclear and particle physics experiments, including the ones performed in Hall B of Jefferson Lab. Dynamically polarized target systems consist of a hydrogenated (polarized protons) or deuterated (polarized neutrons) compound containing paramagnetic centers, such as unpaired electrons, placed in a high magnetic field and cooled to low temperatures, with a B/T ratio of the order of 5 Tesla/Kelvin. In these conditions, the free electron spins can approach polarization of 100%. The high polarization of unpaired electrons is then transferred dynamically to the nucleons by irradiating the target material at frequency near that of electron spin resonance. This technique typically achieves a proton polarization of 80-90%, and a deuteron polarization of 30-40%. The nucleons in the target will be polarized either parallel or anti-parallel to the electron beam direction.

The main systems required to realize DNP are the superconducting magnet to provide a strong (5 T) field, a ^{4}He evaporation refrigerator to maintain the target material at 1 K, a target insert which will house the target material and some additional instrumentation, a microwave system to transfer the polarization to the nucleon spins and a Nuclear Magnetic Resonance (NMR) system to determine the state of polarization.

In CLAS12 the polarizing magnetic field will be provided by the superconducting solenoid of the central detector. In this configuration, the central detector can be used also for polarized target experiments, yielding wide coverage for measurements of multi-hadron final states. The solenoid magnet is in the design stage, and not all parameters are well known at the moment. Some additional correction coils might be necessary to improve the field

uniformity around the target cell. The DNP method requires that the target material is placed in a magnetic field of uniformity $\frac{\Delta B}{B} < 10^{-4}$. The current magnet design provides for such a region of field uniformity in a cylinder of 30 mm in diameter and 100 mm in length. Some properties of the magnet are listed in Table 2.

Type	Superconducting solenoid
Aperture	0.78m warm bore
Central field	2.5-5T
Dimensions	1.10m OD x 0.78m ID x 1.800m long
Region of $\frac{\Delta B}{B} < 10^{-4}$	cylinder: 10 cm long, 3 cm OD

Table 2: CLAS12 solenoid properties

The target cryostat will house the evaporation refrigerator, the target insert and some instrumentation necessary for the microwave and NMR operations. The cryostat needs to be designed to allow its operation in a warm bore magnetic field. A conceptual design of the target cryostat is shown in Fig. 6. The main component of the cryostat is a ^{4}He evaporation refrigerator. The refrigerator is inserted horizontally through a pumping tube between the pumps and the evaporation chamber. One important difference between this design and the previously used polarized target in Hall B is that the refrigerator will be residing along the beam line, so that the amount of materials in the way of the beam needs to be minimized. Liquid helium is supplied to the refrigerator through a transfer line from a dewar located outside of the detector. The liquid enters a copper separator pot, which will have a doughnut-like shape in order not to obstruct the beam path.

In the separator, LHe is separated from the vapor by a sintered filter. The vapor is pumped away cooling the upper heat exchangers, and the liquid is used to cool the target material. There are two needle valves that can transport LHe from the separator pot to the evaporation chamber. The bypass valve allows helium to be transported through a straight tube, going directly to the evaporation chamber, and is used for initial cool down of the target system. The run valve directs helium flow throw a spiral tube, thermally sunk to the copper plated lower hear exchangers. The run valve is typically used during the experiment.

The evaporation chamber will be situated in the bore of the magnet. The central tracker will also be installed in the magnet bore, surrounding the target, and impose constraints on the chamber dimensions. The minimum outer diameter in the present design of the evaporation chamber is 10 cm. This volume will contain the outer vacuum space, heat shield and the evaporation chamber.

The target material will be placed in the cell inside of a cup, with both containers made of hydrogen free plastic. The cup will be attached to a thin aluminum structure that can be inserted through the beam tube. The schematic of the insert is shown on the bottom of Fig. 6. The dimensions of the target cell will be determined by the size of the region of field uniformity, and geometric constraints of the cryostat. The cup will have an opening on the top for the LHe fill, while the cell will have small holes so that the target material will be sitting in a bath of LHe, while also being showered by LHe coming from the run valve. The flow of LHe in the cryostat will be maintained by a series of pumps located outside of the

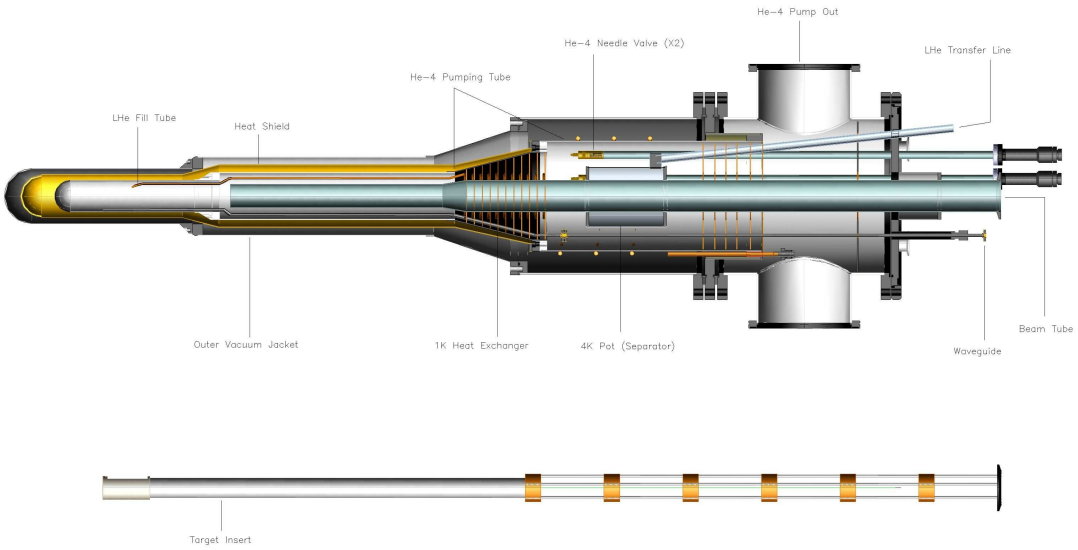

Figure 6: A schematic drawing of the polarized solid target cryostat and target insert for CLAS12.

cryostat. The entrance and exit windows of the target cell and cup could be made out of thin aluminum or Kapton foils. The microwave radiation needed to polarize the target will be guided through a designated waveguide inserted through the upstream entrance window of the cryostat. The guide will have a slit directly underneath the target cup, providing continuous microwave radiation directed at the target cell. With this arrangement, the target cup will act as a resonating cavity.

Ammonia and deuterated ammonia will be used as target material with the electron beam and CLAS12. In order to determine the dilution factor (fraction of events originating from unpolarized target materials) for each process with sufficiently high accuracy, about 20% of the runnig time will be devoted to measurements with carbon, nitrogen, and helium. To determine the proton to deuteron and deuteron to carbon cross section ratios, we will need a few days of running with the same magnetic fields and target position as the present experiment, but with gas or liquid hydrogen and deuterium targets. We anticipate that this can be scheduled in conjunction with other planned experiments with CLAS12.

For measurements on polarized deuterium, we may choose to use ^{6}LiD or HD as the target material, rather than ND_3. Both targets provide a very substantially higher dilution factor, and therefore substantially smaller statistical and systematic errors, for a given target

Name	Material	Dimensions
Outer Vacuum Jacket	Al	0.5 mm
Heat Shield	Al	0.5 mm
Cup Wall	Kel-F	0.5 mm
Cup/Cell Windows	Al	0.025 mm
Cell	Kel-F/torlon	0.3 mm

Table 3: New cryostat and insert design parameters

Chemical Structure	$NH_3(ND_3)$
Target Diameter	up to 30 mm
Target Length	up to 100 mm
Density	0.917(1.056) g/cm^3
Dilution Factor	$\approx 0.15(0.22)$
Packing Factor	≈ 0.6

Table 4: Some Parameters of the Ammonia Targets

polarization and luminosity. In the case of ^{6}LiD, the good dilution factor arises through the assumption that ^{6}LiD can be regarded to first approximation as an unpolarized alpha particle bound with a polarized deuteron. The extent to which this approximation is valid will be tested in the approved 6 GeV experiment E07-011 in Hall C. The frozen spin HD target has been recently approved by DOE to be transferred to JLab for a program of photoproduction experiments. Planned tests will show if this target can withstand the heat load of a sufficiently high beam current to make this target material competitive with ND_3 or ^{6}LiD. If so, the very good dilution factor (over 50%) and lack of nuclear corrections from polarized nitrogen or lithium will make this the target of choice.

The target polarization will be monitored during the run via the NMR system, in the field of solenoid magnet. The calibration of the proton NMR can be done by measurements of polarization in thermal equilibrium, taken with the polarizing magnet.

2.3 The Data Set and analysis

We will run with a beam of about 10 nA on a 3 cm long ammonia target, resulting in a luminosity of 10^{35}/cm^{2}s. The beam will be rastered over the diameter of the polarized target (about 3 cm) to minimize the dose density (we will need at most one anneal every other day under these conditions). We assume a beam polarization of 0.85, which has been routinely achieved in recent experiments running at Jefferson Lab. The beam helicity will be flipped in a pseudo-random pattern every 33 ms. We will use the standard Hall B beam devices to monitor and stabilize the beam intensity and position. In particular, we will reduce any helicity-correlated beam asymmetries to less than 10^{-3}.

The first-level trigger will consist of a coincidence between the high-threshold Cerenkov counter and a signal above threshold (corresponding to at least 1 GeV deposited) in the

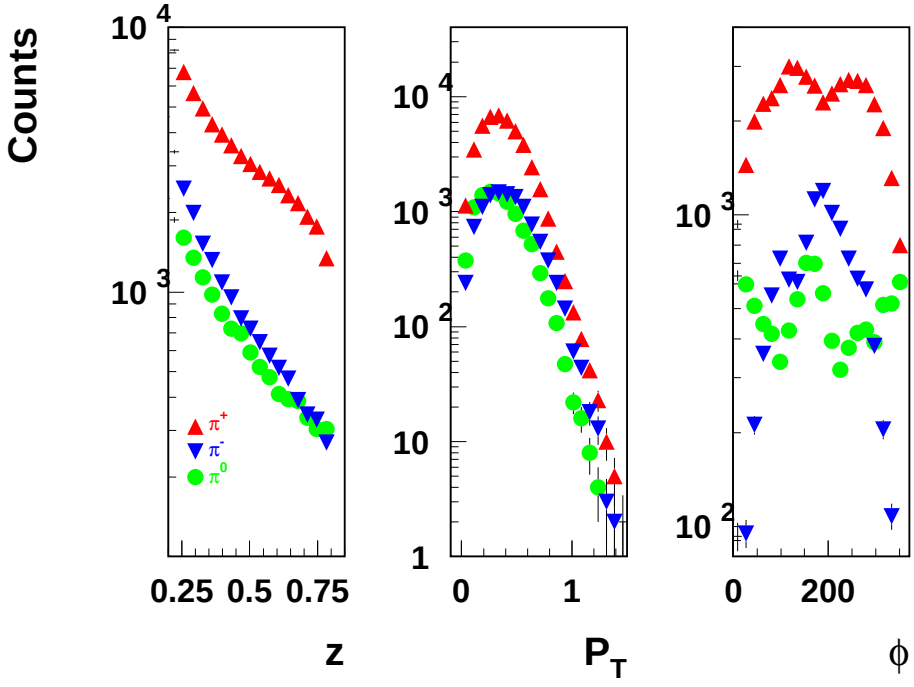

Figure 7: Kinematic coverage in the SIDIS region of the proposed experiment.

electromagnetic calorimeter in the same sector. This trigger will be highly specific for high-energy electrons, with little contamination from pions and other particles. In the case of too high background, we can also implement a level 2 trigger which requires a electron candidate track in the drift chambers of the same sector as the level 1 trigger. This has already been developed for the present CLAS. The total event rate in the DIS region for this experiment is expected to be around 2000 Hz above $Q^2 = 1$ GeV^2. Estimates of the total trigger rate are around 20 kHz. A data acquisition rate of 10 kHz has already been achieved with today's technology for the present CLAS DAQ, so that the required data acquisition rate for this experiment is a rather modest extrapolation.

In Fig.7 we show the kinematic coverage in the DIS region expected from the proposed experiment with 11 GeV beam and CLAS12. Clearly this will constitute a substantial increase over the existing Jefferson Lab data in both x and Q^2 (maximum Q^2 of 5 GeV^2 and x between 0.2 and 0.6), while the precision of the expected data will be far superior to existing DIS experiments from other labs.

The data will consist of the number of counts for beam helicity anti-parallel (N^+) and parallel (N^-) to the longitudinal target polarization, each normalized to the dead-time corrected integrated beam charge. We will subtract from these rates the backgrounds from misidentified pions (which can be obtained from fits to the distribution of photo-electrons in the high-threshold Cerenkov counter and the measured ratio of visible energy deposited in the electromagnetic calorimeter to the measured momentum) and from electrons coming

from pair-symmetric decays (e.g., $\pi^0 \to e^+e^-$ or $\pi^0 \to \gamma e^+e^-$ as well as $\gamma \to e^+e^-$ conversions). From the corrected counts, we will form the ratio $A_{||}^{raw} = (N^+ - N^-)/(N^+ + N^-)$. This ratio has to be divided by the product of beam and target polarization and the dilution factor (the fraction of counts coming from the polarized nuclei in the target to the total).

The dilution factor can be calculated from a detailed model of the target content and a parametrization of the world data on unpolarized structure function for nucleons and nuclei (^{15}N, ^{4}He, and C and Al foils) in the target, including radiative effects. The only ingredient needed is the packing fraction (the fraction of the cell volume occupied by the ammonia beads), which can be extracted by comparing the rate from ammonia to that from an auxiliary carbon target. Additional measurements on empty and liquid-helium only targets will also be needed. Past experience with the EG1 experiment in Hall B have shown that a typical error of 3% on the dilution factor can be achieved [64]. An additional correction for the small polarization in ^{15}N and contamination by ^{14}N and, in the case of the deuterated ammonia, H, will be applied as well.

2.3.1 Azimuthal asymmetries

The beam (P_B) and target (P_T) polarization will be independently measured using Möller scattering and NMR, respectively. However, we can extract the product $P_B * P_T$ with higher precision directly from our data, by measuring the asymmetry of elastic (quasi-elastic) scattering $\vec{p}(\vec{e}, e'p)$ ($\vec{d}(\vec{e}, e'p)$) from our NH_3 (ND_3) targets, respectively. We did a full simulation of this method, including radiative effects, CLAS12 acceptance and expected beam parameters. We find that the uncertainty on $P_B * P_T$ for the proton will be about 1% and on the deuteron about 3%.

Measurements of average moments $\langle W(\phi)\rangle_{UL} = \int \sigma_{UL}(\phi) W(\phi) d\phi / \int \sigma(\phi) \sin^2\phi d\phi$ ($W(\phi) = \sin\phi, \sin 2\phi$) of the cross section $\sigma_{UL}^{W(\phi)}$ will single out corresponding terms in the cross section. Thus the $\sin\phi$ SSA of the cross section for longitudinally polarized target and unpolarized beam is defined as:

$$A_{UL}^{\sin\phi} = \frac{\langle \sin\phi \rangle_{UL}}{\langle \sin^2\phi \rangle_{UU}} = \frac{1}{P^{\pm} N^{\pm}} \frac{\sum_{i=1}^{N^{\pm}} \sin\phi_i}{\sum_{i=1}^{N^{\pm}} \sin^2\phi_i}, \tag{19}$$

where $P^{\pm}$ and $N^{\pm}$ are the polarization and number of events for $\pm$ helicity state, respectively. For spin-dependent moments this is equivalent to the corresponding spin asymmetries A_{UL}^{W}. The final asymmetry is defined by the weighted average over two independent measurements for both helicity states or by fitting with corresponding azimuthal dependences ($\sin\phi, \sin 2\phi$) the spin asymmetries binned in the azimuthal angle.

2.3.2 Flavor decomposition and helicity distributions

The double spin asymmetry in SIDIS for charged and neutral pions is sensitive to the polarized parton densities through the different flavor sensitivities tagged by the pion charge.

In terms of improved parton densities, an important observation is that the systematic errors largely cancel in the ratio of g_1/F_1 for SIDIS pion production to the values for inclusive production. Therefore this ratio, which is unity in LO QCD for π^0 or the sum of π^+ and π^- if sea quark contributions and gluon radiation are ignored, can be measured with high

statistical and systematic precision (for example with relative errors of 3% in each of 5 x bins). The deviations from unity which are expected due to different sea quark contributions and gluon radiation in the evolution equations can therefore be determined with unprecedented accuracy.

The depolarization factor D depends on the ratio R of longitudinal to transverse photo absorption cross sections, which is well known after a series of detailed experiments in Jefferson Lab's Hall C.

3 Expected Results

3.1 Simulation

The expected number of counts and corresponding statistical errors in the following sections are based on a full simulation of inclusive and semi-inclusive inelastic scattering with the CLAS12 acceptance folded in. Events were generated with the clas12DIS generator [65]. This generator is basically an implementation of the LUND Monte Carlo package called PEPSI (Polarized Electron-Proton Scattering Interactions) [51]. It is based on polarized and unpolarized parton distribution functions and the LUND string model for hadronization, and has been tested successfully against several low-Q^2 experiments with 5.7 GeV beam at Jefferson Lab.

A fast Monte Carlo simulation program has been used to define the acceptance and resolution of the CLAS12 detector with all of the standard (base) equipment in place. The events generated by clas12DIS are used as input and all particles are followed through all detector elements. The results of our simulation have been cross-checked with direct cross section calculations and a simple geometric acceptance model.

The resolution of the detector is simulated by a simple smearing function which modifies a particle's track by a random amount in momentum and angles according to a Gaussian distribution of the appropriate width. The amount of smearing follows the design specifications of the CLAS12 detector. The resolution in x_B varies between $0.01 < \sigma_x < 0.035$ and is therefore finer than our planned x bin size of 0.05 in all cases. Extracted from MC double spin asymmetries and corresponding helicity distributions are shown on Fig.8.

A full Monte Carlo simulation (GEANT-based) of CLAS12 with all resolution effects will be used to determine the effective mean x (and Q^2) for each x-bin we will use to bin our data so we can accurately extract the x-dependence of the measured asymmetries.

3.2 Statistical and systematic errors

The proposed spin asymmetry measurement is rather insensitive to uncertainties in acceptances and charge normalization. The main systematic error is due to possible contamination of the single pion sample with pions from decays of exclusive vector mesons. Other sources of systematic errors include the beam and target polarizations, dilution factor the longitudinal to transverse photo absorption cross section ratio, $R(x, Q^2)$. The main sources of systematic errors in measurements of single and double spin asymmetries are listed in the Table 5. These errors are all scale errors, so are proportional to the size of the measured asymmetry.

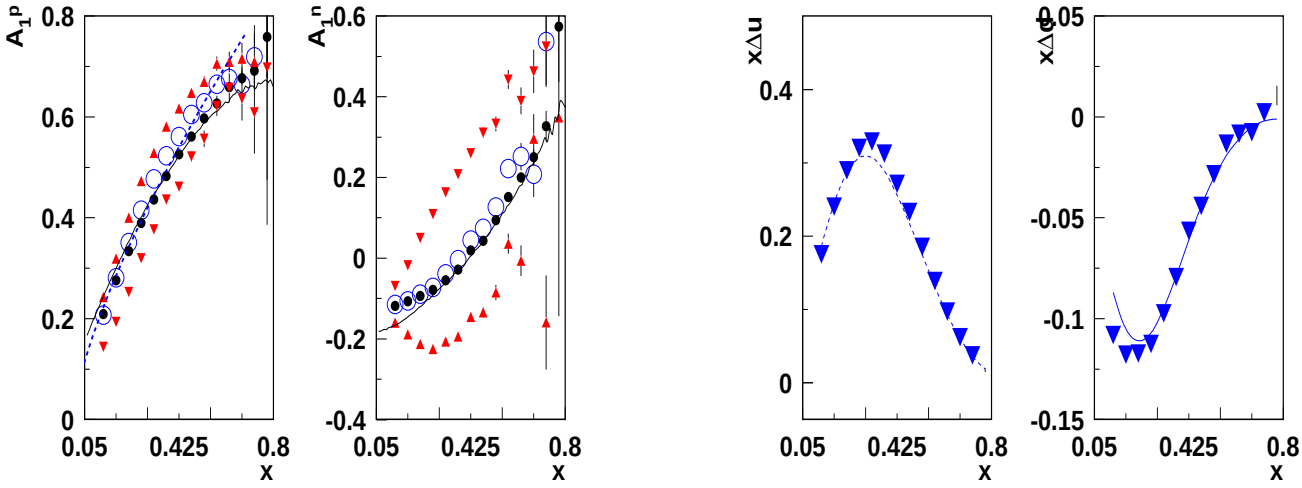

Figure 8: The double spin asymmetries on proton (left) and neutron(right) targets, for π^+ (triangles up), π^- (triangles down) π^0 (empty circles), inclusive electrons (filled circles). The solid line is the calculation using GRV98 and GRSV PDFs (at scale Q^2=2) and the dashed line is a simple parametrization ($A_1 = x^{0.72}$). The right panel shows extracted Δu(left) and Δd (right) using only the A_1^p on proton and neutron for π^0, using a simple partonic expression. The solid line is the calculation using GRV98 and GRSV PDFs (at scale Q^2=2). The s-quark contribution is neglected.

Table 5: Uncertainties for asymmetry measurements.

Item	A_1^p	$A_{UL}^{\sin\phi}$	$A_{UL}^{\sin 2\phi}$
beam x target polarization	2%	-	-
target polarization	-	3%	3%
depolarization and R	4%	-	-
dilution factor	3%	3%	3%
radiative corrections	3%	3%	3%
fitting procedure	-	4%	5%
transverse (to γ^*) spin effects	3%	3%	-%

The total uncertainty is expected to be less than 10% of the measured SSA. For the $\sin 2\phi$ SSA, statistical uncertainties are expected to dominate the total uncertainty.

Studies of other sources of systematics, related to physics background, including target fragmentation, semi-exclusive processes, exclusive vector meson contributions and higher twist require the data of this measurement.

We base our predicted statistical errors in the following sections on the assumption of running 30 days on NH_3 and 50 days on ND_3. The number of days was chosen to achieve a statistical error that is not significantly larger than the systematical error at the highest x and P_T points. More days on deuterium than the proton ensures that both have the same statistical error at large P_T and optimizes the error on extracted quantities like $h_{1L}^{\perp u,d}$ and $\Delta d_v/d_v$.

For our estimate of the total systematic error, we have added the systematic errors from

the various contributions discussed in the previous Section in quadrature. They are listed in Table 5. Note that some systematic errors (like the overall scale error coming from the beam and target polarization) affect the extraction of PDFs or higher twist contributions less than point-to-point errors, which typically are smaller. Additional contributions to systematic error of measured asymmetries will come from uncertainties of unpolarized structure functions and also attenuation of hadrons in nuclear environment, which are a subject of a separate study (PAC-30 proposal on nuclei)

3.3 Results

The proposed experiment will simultaneously collect data on $\vec{p}, \vec{d}(\vec{e}, e'\pi^{+,0,-})$. The charged pions will be detected in the forward spectrometer and the central tracker of CLAS12 in coincidence with the scattered electrons. The following predicted results were obtained with a full simulation of the hadronization process [51] and the acceptance of CLAS12 for all particles.

In addition to the backgrounds already discussed earlier, for the pion production channel we will have to consider contributions from diffractive vector meson production (e.g., $\rho \to \pi\pi$) and the radiative tail on exclusive pion production. For the NLO analysis, we also need to know the unpolarized cross section for SIDIS pion production, which will be measured in several Hall C experiments (both with the present 6 GeV beam and also with the upgraded CEBAF). The contributions to the systematic error from these backgrounds requires a detailed analysis once the requisite data are in hand, but experience with EG1 data from CLAS at 6 GeV show that one can avoid most of them by judicious choice of kinematic cuts.

Projections for the resulting kinematic dependence of the leading-twist SSA are shown in Fig. 9. Calculations were done using $h_{1L}^{\perp}$ from the chiral quark soliton model evolved to Q^2=1.5 GeV^2 [20], f_1 from GRV95 [52], and D_1 from Kretzer, Leader, and Christova [53]. Two different curves correspond to $H_1^{\perp u\to\pi^-}/H_1^{\perp u\to\pi^+} = 0, -1.2$ [61]. Corresponding projected error bars for the Mulders TMD parton distribution are shown in Fig. 9. Estimates are performed assuming the so-called "Lorentz-invariance relations" that connect $h_{1L}^{\perp}$ with h_1 [34]. This measurement will check out experimentally to which extent such relations actually hold [54, 55].

Proposed measurements of SSAs in SIDIS will pin down the corresponding TMD distribution and will constrain the ratio of favored to unfavored polarized fragmentation functions. The new data will also allow a more precise test of the factorization ansatz and the investigation of the Q^2 dependence of $\sin 2\phi$, $\sin\phi$, and $\cos\phi$ asymmetries. This will enable us to study the leading-twist and higher-twist nature of the corresponding observables [35, 66, 41, 21, 22, 23, 14].

Measurement of the P_T dependence of the Kotzinian-Mulders-asymmetry will also allow for checking of the predictions of a unified description of SSA by Ji and collaborators [13, 67] and for study of the transition from a non-perturbative to a perturbative description. The $\sin 2\phi$ asymmetry for semi-inclusive deep inelastic scattering in the kinematic regions of `CLAS12` is predicted to be significant (a few percent on average) and tends to be larger in the large-x and large-z region.

The combined analysis of the future `CLAS12` data on $\langle \sin 2\phi \rangle$ and of the previous HERMES

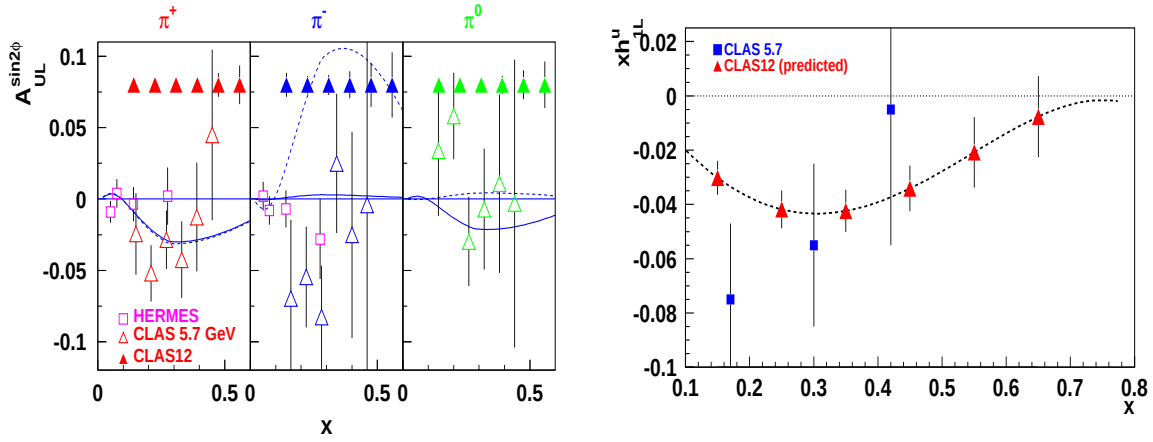

(a) (b)

Figure 9: (Left) The projected x-dependence of the target SSA at 11 GeV. The triangles illustrate the expected statistical accuracy. The open squares and triangles show the existing measurement of the Mulders TMD from HERMES and the preliminary results from CLAS 5.7 GeV EG1 data sets, respectively. The curves are calculated using Ref. [61]. (Right) Projection for the Mulders distribution function for the u-quark from the π^+ SSA from CLAS12 (predicted) compared with the CLAS EG1 data set at 5.7 GeV.

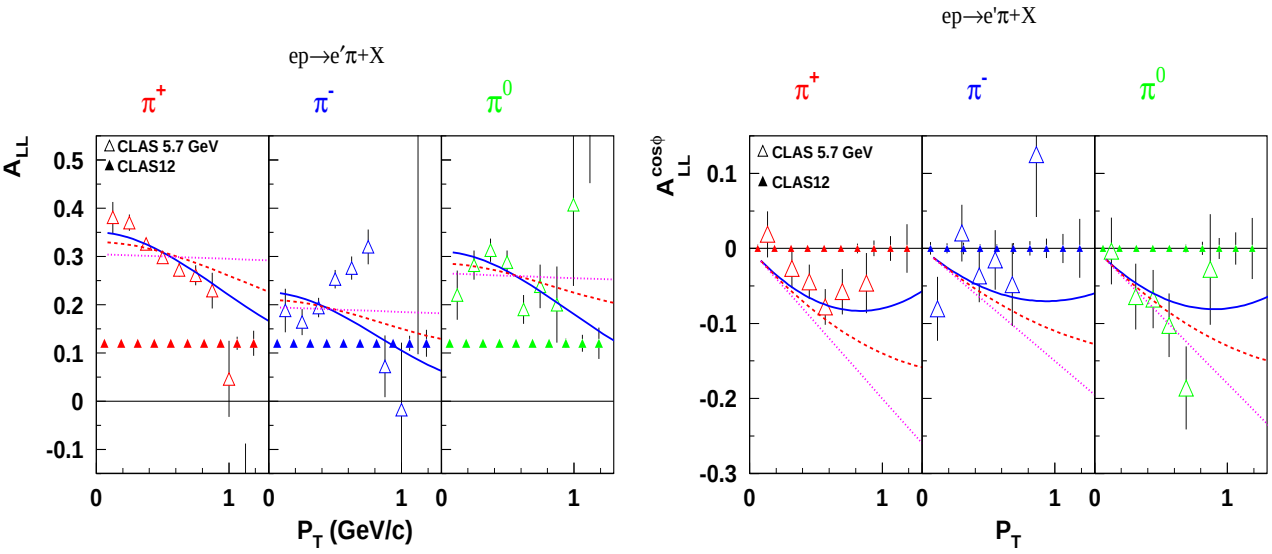

Figure 10: The double spin asymmetry A_{LL} (left) and its $\cos\phi$ moment (right) for the NH_3-target as a function of the transverse momentum of hadrons, P_T, averaged in the $0.4 < z < 0.7$ range.

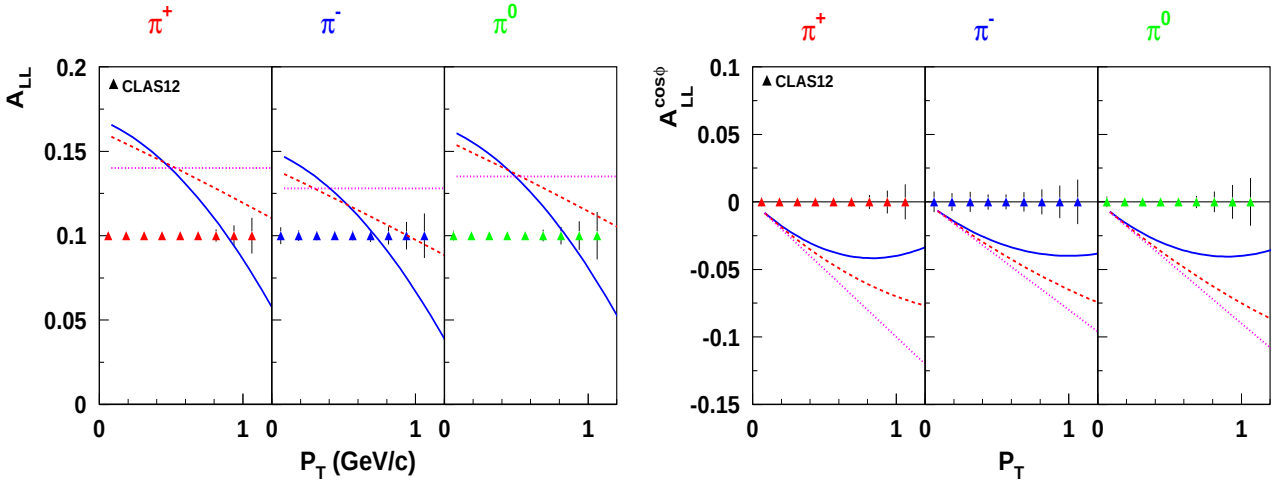

Figure 11: The double spin asymmetry A_{LL} (left) and its $\cos\phi$ moment (right) for the ND_3-target as a function of the transverse momentum of hadrons, P_T, averaged in the $0.4 < z < 0.7$ range.

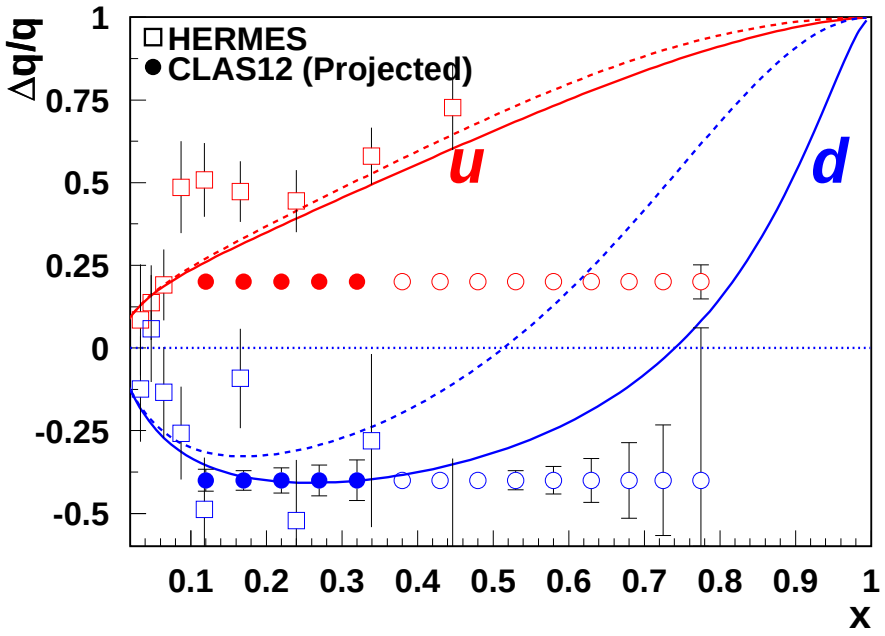

Figure 12: The polarization of valence quarks ($\frac{\Delta d_V}{d_V}$) in the nucleon. The filled symbols are for the SIDIS data only and open symbols are for DIS data neglecting sea contributions. The curves are pQCD based predictions with (solid) and without (dashed) OAM contributions [29].

measurements in the high-Q^2 domain (where higher-twist effects are less significant) will provide information on the Mulders function, shedding light on the correlations between transverse spin and transverse momenta of quarks. Significantly increasing the kinematic coverage at large Q^2 and P_T, CLAS12 (see Fig. 9) will map the quark TMDs in the valence region allowing study of the transition from a non-perturbative description at small P_T to a perturbative description at large P_T.

Table 6 contains the expected counts in different kinematic bins for the hydrogen target for each of the pion states. At lower x, this very large data set allows us to further subdivide the data into bins in p_T and z. Once in hand, these data will be combined with existing SIDIS data from HERMES, COMPASS and RHIC for a full NLO analysis. From this analysis, we will extract the polarized PDFs for each quark and antiquark flavor in the region $0.1 \leq x \leq 0.8$.

Projections for the resulting P_T-dependence of the double spin asymmetries for all three pions are shown in Fig. 10 and Fig. 11 for NH_3 and ND_3 targets respectively. These measurements using unfolding of Eqs.17-18 would allow access the k_T-distributions of u and d-quarks aligned and anti-aligned with the spin of the nucleon. Integrated over the transverse momentum the data will be also used to extract the k_T-integrated standard PDFs.

To illustrate the expected precision for the flavor-separated quark polarization from the proposed experiment, we used the approach of Eq. 13 to determine $\frac{\Delta d_V}{d_V}$ from the predicted rates of π^+ and π^- production off proton and deuteron targets as a function of relative beam and target spin. The results are shown in Fig. 12, together with existing HERMES SIDIS results and the inclusive data from Hall A. The error bars in this plot were calculated using a fit for the ratio $\frac{d}{u}$ from NMC fit. We assume that in the future $\frac{d}{u}$ will be known to about 5-10% in the region covered by our data (see the "BoNuS12" proposal to PAC30). The large error bars at small x are for only SIDIS as DIS data will not be used in k_T-dependent studies.

The expected data shown in Figure 12 are comparable with the precision achievable from the inclusive DIS measurement in particular at somewhat lower x where the contribution from anti-quarks is no longer negligible, only the SIDIS method can cleanly extract the valence quark behavior. In addition, SIDIS data depend in a somewhat different way on the assumption of isospin symmetry than DIS data, so a comparison between the two data sets could potentially uncover large violations of that symmetry. Most importantly the SIDIS measurements provide access to transverse momentum dependence of helicity distributions not accessible in inclusive DIS. The SIDIS measurements proposed here will cover the gap between low-x covered by HERMES and inclusive data at large-x from JLab inclusive experiments allowing a global fit to extract the contribution from OAM.

Measured single and double spin asymmetries for all pions in a large range of kinematic variables (x_B, Q^2, z, $P_\perp$ and ϕ) combined with measurements with unpolarized target will provide detailed information on flavor and polarization dependence of transverse momentum distributions of quarks in valence region and in particular on the x_B and k_T dependence of leading TMD parton distribution functions of u and d quarks. Measurements of spin and azimuthal asymmetries across a wide range of x, z, Q^2 and P_T would allow to perform detailed tests of QCD dynamics in valence region.

Measurements of semi-inclusive processes combined with inclusive and exclusive measurements with upgraded JLab will allow to study the quark structure of nucleon with

Table 6: Counts in bins in Q^2 and x_B, z and $P_\perp$.

x_B	Q^2(GeV^2)	z	$p_\perp$(GeV)	π^+	π^-	π^0
0.12	1.87	0.65	0.06	59592	2592	44544
0.12	1.87	0.65	0.18	165864	14520	1000056
0.12	1.87	0.65	0.31	238632	22104	115704
0.12	1.87	0.65	0.43	223752	29256	96144
0.12	1.87	0.65	0.56	163608	28272	70560
0.12	1.87	0.65	0.68	99960	23688	42576
0.12	1.87	0.65	0.81	49488	12024	19008
0.12	1.87	0.65	0.93	20832	5928	7944
0.12	1.87	0.65	1.06	8040	2760	3216
0.12	1.87	0.65	1.18	2784	1080	1968
0.12	1.87	0.65	1.31	1104	480	696
0.12	1.87	0.65	1.43	576	240	192
0.17	2.66	0.55	0.06	51192	3264	30912
0.17	2.66	0.55	0.18	140400	14328	78744
0.17	2.66	0.55	0.31	176280	23448	93816
0.17	2.66	0.55	0.43	160608	28632	77304
0.17	2.66	0.55	0.56	114048	27120	51696
0.17	2.66	0.55	0.68	65208	17976	28512
0.17	2.66	0.55	0.81	29520	9096	12504
0.17	2.66	0.55	0.93	11904	3936	5088
0.17	2.66	0.55	1.06	3912	1536	2208
0.17	2.66	0.55	1.18	1776	960	672
0.17	2.66	0.55	1.31	744	240	240
0.17	2.66	0.55	1.43	336	120	120
0.22	3.78	0.55	0.06	25800	1008	11616
0.22	3.78	0.55	0.18	65256	6096	34032
0.22	3.78	0.55	0.31	80904	9360	41520
0.22	3.78	0.55	0.43	72120	12144	34272
0.22	3.78	0.55	0.56	50256	11208	22128
0.22	3.78	0.55	0.68	29040	7128	12456
0.22	3.78	0.55	0.81	12936	4104	5424
0.22	3.78	0.55	0.93	4488	1536	1992
0.22	3.78	0.55	1.06	1728	648	816
0.22	3.78	0.55	1.18	648	288	288
0.22	3.78	0.55	1.31	240	24	144
0.22	3.78	0.55	1.43	168	120	48
0.27	3.78	0.65	0.06	35952	6024	10488
0.27	3.78	0.65	0.18	100272	13032	22920
0.27	3.78	0.65	0.31	118104	12360	33696
0.27	3.78	0.65	0.43	98376	11112	31272
0.27	3.78	0.65	0.56	59784	9888	22368
0.27	3.78	0.65	0.68	31920	6504	12768
0.27	3.78	0.65	0.81	12840	3336	5928
0.27	3.78	0.65	0.93	4848	1632	2616
0.27	3.78	0.65	1.06	1296	600	888
0.27	3.78	0.65	1.18	552	216	312
0.27	3.78	0.65	1.31	144	72	24
0.27	3.78	0.65	1.43	24	24	48
0.32	5.40	0.65	0.06	15216	1488	3024
0.32	5.40	0.65	0.18	37368	3144	8880
0.32	5.40	0.65	0.31	43632	4200	13536
0.32	5.40	0.65	0.43	35664	3888	13296
0.32	5.40	0.65	0.56	24720	3432	8808
0.32	5.40	0.65	0.68	13056	1848	5304
0.32	5.40	0.65	0.81	4752	1152	2640
0.32	5.40	0.65	0.93	1632	504	1032
0.32	5.40	0.65	1.06	576	288	384
0.32	5.40	0.65	1.18	144	48	120
0.52	7.30	0.55	0.06	4344	984	1416
0.52	7.30	0.55	0.18	11880	2136	3816
0.52	7.30	0.55	0.31	14448	1872	4344
0.52	7.30	0.55	0.43	11184	1440	3792
0.52	7.30	0.55	0.56	6144	984	2232
0.52	7.30	0.55	0.68	2904	768	1200
0.52	7.30	0.55	0.81	816	144	456
0.52	7.30	0.55	0.93	288	96	144
0.52	7.30	0.55	1.06	72	24	24
0.57	9.50	0.65	0.06	744	48	96
0.57	9.50	0.65	0.18	1296	168	432
0.57	9.50	0.65	0.31	1512	192	408
0.57	9.50	0.65	0.43	1512	240	360
0.57	9.50	0.65	0.56	528	168	336
0.57	9.50	0.65	0.68	552	48	240
0.57	9.50	0.65	0.81	168	48	144
0.57	9.50	0.65	0.93	48	24	24
0.62	7.30	0.55	0.06	984	360	576
0.62	7.30	0.55	0.18	2856	1248	1296
0.62	7.30	0.55	0.31	3552	1296	1584
0.62	7.30	0.55	0.43	3240	504	816
0.62	7.30	0.55	0.56	1632	528	528
0.62	7.30	0.55	0.68	1152	216	264
0.62	7.30	0.55	0.81	288	72	96
0.62	7.30	0.55	0.93	48	48	48

Time	Activity
3 days	Commissioning: Beam raster set up, trigger optimization, low energy calibration runs
30 days	Production data taking on NH_3
50 days	Production data taking on ND_3
3 days (1 1/2 hours every other day)	Target anneals and/or target changes
10 days (intermittent with production data)	Calibration runs on ^{12}C and empty target
5 days	Production runs on ^{15}N
2 day (1 hour every other day – concurrent with anneals)	Möller polarimeter runs

Table 7: Requested beam time broken down by activity.

unprecedented detail. Understanding of spin-orbit correlations, together with independent measurements related to the spin and orbital angular momentum of the quarks will help construct a more complete picture of the nucleon in terms of elementary quarks and gluons going beyond the simple collinear partonic representation.

4 Summary and Request

The proposed set of measurements on polarized proton and deuteron targets will yield a comprehensive set of single and double spin asymmetries and corresponding distribution and fragmentation functions in a wide range of x, Q^2, z and P_T. Our data, combined with the data from HERMES, COMPASS and BELLE, will allow us to extract leading twist TMD parton distributions $g_1(x, k_T)$ and $h_{1L}(x, k_T)$. Measurements of semi-inclusive processes combined with inclusive and exclusive measurements with an upgraded JLab will allow us to study the quark structure of the nucleon with unprecedented detail. Understanding of spin-orbit correlations, together with independent measurements related to the spin and orbital angular momentum of the quarks, will help to construct a more complete picture of the nucleon in terms of elementary quarks and gluons going beyond the simple collinear partonic representation. Finally, we can improve considerably on our knowledge of higher twist contributions to different azimuthal moments of spin dependent cross section.

To achieve this goal, we request a total of 103 days of beam time with an 11 GeV, 10 nA highly polarized electron beam in Hall B. The breakdown of this beam time is shown in Table 7. The number of days requested was chosen to optimize the impact of our data and to make the systematic and statistical errors roughly equal for the highest x data points.

We want to conclude by noting that while this experiment requires a substantial commitment of beam time (103 days total), most of the time we will simultaneously take data with already approved experiment to study the inclusive DIS [63]. In addition, the proposed experiment will yield data on single (target and beam) spin asymmetries in SIDIS which can provide constraints on the higher-twist nucleon structure functions and provide complementary to transverse target information on spin-orbit correlations (the LOI submitted to PAC-30 [68]).

References

[1] European Muon, J. Ashman et al., Phys. Lett. B206 (1988) 364.

[2] Spin Muon (SMC), D. Adams et al., Phys. Rev. D56 (1997) 5330, hep-ex/9702005.

[3] E143, K. Abe et al., Phys. Rev. D58 (1998) 112003, hep-ph/9802357.

[4] E155, P.L. Anthony et al., Phys. Lett. B458 (1999) 529, hep-ex/9901006.

[5] HERMES, K. Ackerstaff et al., Phys. Lett. B464 (1999) 123, hep-ex/9906035.

[6] HERMES, A. Airapetian et al., Phys. Rev. D71 (2005) 012003, hep-ex/0407032.

[7] CLAS, R. Fatemi et al., Phys. Rev. Lett. 91 (2003) 222002, nucl-ex/0306019.

[8] S.J. Brodsky, D.S. Hwang and I. Schmidt, Phys. Lett. B530 (2002) 99, hep-ph/0201296.

[9] J.C. Collins, Phys. Lett. B536 (2002) 43, hep-ph/0204004.

[10] X. Ji and F. Yuan, Phys. Lett. B543 (2002) 66, hep-ph/0206057.

[11] A.V. Belitsky, X. Ji and F. Yuan, Nucl. Phys. B656 (2003) 165, hep-ph/0208038.

[12] D. Boer, P.J. Mulders and F. Pijlman, Nucl. Phys. B667 (2003) 201, hep-ph/0303034.

[13] X. Ji, J. Ma and F. Yuan, Phys. Rev. D71 (2005) 034005, hep-ph/0404183.

[14] J.C. Collins and A. Metz, Phys. Rev. Lett. 93 (2004) 252001, hep-ph/0408249.

[15] X.d. Ji, J.P. Ma and F. Yuan, Nucl. Phys. B652 (2003) 383, hep-ph/0210430.

[16] D.W. Sivers, Phys. Rev. D43 (1991) 261.

[17] M. Anselmino and F. Murgia, Phys. Lett. B442 (1998) 470, hep-ph/9808426.

[18] S.J. Brodsky, D.S. Hwang and I. Schmidt, Nucl. Phys. B642 (2002) 344, hep-ph/0206259.

[19] J.C. Collins, Nucl. Phys. B396 (1993) 161, hep-ph/9208213.

[20] A.V. Efremov, K. Goeke and P. Schweitzer, Phys. Rev. D67 (2003) 114014, hep-ph/0208124.

[21] A. Afanasev and C.E. Carlson, (2003), hep-ph/0308163.

[22] F. Yuan, Phys. Lett. B589 (2004) 28, hep-ph/0310279.

[23] A. Metz and M. Schlegel, Eur. Phys. J. A22 (2004) 489, hep-ph/0403182.

[24] HERMES, A. Airapetian et al., Phys. Rev. Lett. 84 (2000) 4047, hep-ex/9910062.

[25] HERMES, A. Airapetian, (2006), hep-ex/0612059.

[26] CLAS, H. Avakian et al., Phys. Rev. D69 (2004) 112004, hep-ex/0301005.

[27] HERMES, A. Airapetian et al., Phys. Rev. Lett. 94 (2005) 012002, hep-ex/0408013.

[28] COMPASS, V.Y. Alexakhin et al., Phys. Rev. Lett. 94 (2005) 202002, hep-ex/0503002.

[29] H. Avakian et al., (2007), arXiv:0705.1553 [hep-ph].

[30] R. Jakob, P.J. Mulders and J. Rodrigues, (1997), hep-ph/9707340.

[31] M. Anselmino et al., Phys. Rev. D74 (2006) 074015, hep-ph/0608048.

[32] A.M. Kotzinian and P.J. Mulders, Phys. Rev. D54 (1996) 1229, hep-ph/9511420.

[33] A. Kotzinian, Nucl. Phys. B441 (1995) 234, hep-ph/9412283.

[34] P.J. Mulders and R.D. Tangerman, Nucl. Phys. B461 (1996) 197, hep-ph/9510301.

[35] J. Levelt and P.J. Mulders, Phys. Lett. B338 (1994) 357, hep-ph/9408257.

[36] D. Boer and P.J. Mulders, Phys. Rev. D57 (1998) 5780, hep-ph/9711485.

[37] R.D. Tangerman and P.J. Mulders, Phys. Rev. D51 (1995) 3357, hep-ph/9403227.

[38] S.J. Brodsky and F. Yuan, Phys. Rev. D74 (2006) 094018, hep-ph/0610236.

[39] P.V. Pobylitsa, (2003), hep-ph/0301236.

[40] A. Bacchetta et al., Phys. Rev. D65 (2002) 094021, hep-ph/0201091.

[41] A.M. Kotzinian et al., (1999), hep-ph/9908466.

[42] Belle, K. Abe et al., Phys. Rev. Lett. 96 (2006) 232002, hep-ex/0507063.

[43] HERMES, A. Airapetian et al., Phys. Rev. D64 (2001) 097101, hep-ex/0104005.

[44] M. Anselmino et al., (2007), hep-ph/0701006.

[45] HERMES, A. Airapetian et al., Phys. Rev. Lett. 84 (2000) 2584, hep-ex/9907020.

[46] Spin Muon (SMC), B. Adeva et al., Phys. Rev. D70 (2004) 012002, hep-ex/0402010.

[47] COMPASS, E.S. Ageev et al., Phys. Lett. B633 (2006) 25, hep-ex/0511028.

[48] PHENIX, A. Adare, (2007), arXiv:0704.3599 [hep-ex].

[49] E. Leader, A.V. Sidorov and D.B. Stamenov, Int. J. Mod. Phys. A13 (1998) 5573, hep-ph/9708335.

[50] L.L. Frankfurt, L. Mankiewicz and M.I. Strikman, Z. Phys. A334 (1989) 343.

[51] L. Mankiewicz, A. Schafer and M. Veltri, Comput. Phys. Commun. 71 (1992) 305.

[52] M. Gluck et al., Phys. Rev. D53 (1996) 4775, hep-ph/9508347.

[53] S. Kretzer, E. Leader and E. Christova, Eur. Phys. J. C22 (2001) 269, hep-ph/0108055.

[54] K. Goeke et al., Phys. Lett. B567 (2003) 27, hep-ph/0302028.

[55] K. Goeke, A. Metz and M. Schlegel, Phys. Lett. B618 (2005) 90, hep-ph/0504130.

[56] CLAS, H. Avakian et al., AIP Conf. Proc. 792 (2005) 945, nucl-ex/0509032.

[57] A. Afanasev, C.E. Carlson and C. Wahlquist, Phys. Lett. B398 (1997) 393, hep-ph/9701215.

[58] S.J. Brodsky and S.D. Drell, Phys. Rev. D22 (1980) 2236.

[59] S.J. Brodsky, M. Burkardt and I. Schmidt, Nucl. Phys. B441 (1995) 197, hep-ph/9401328.

[60] M. Gockeler et al., Nucl. Phys. Proc. Suppl. 153 (2006) 146, hep-lat/0512011.

[61] A.V. Efremov, K. Goeke and P. Schweitzer, Czech. J. Phys. 55 (2005) A189, hep-ph/0412420.

[62] Spin Muon, B. Adeva et al., Phys. Lett. B420 (1998) 180, hep-ex/9711008.

[63] Jefferson Lab Hall B, S. Kuhn et al., PAC30 Proposal (2006).

[64] CLAS, K.V. Dharmawardane et al., Phys. Lett. B641 (2006) 11, nucl-ex/0605028.

[65] H. Avakian and P. Bosted., (2006).

[66] R.L. Jaffe and X.D. Ji, Nucl. Phys. B375 (1992) 527.

[67] X. Ji et al., Phys. Rev. D73 (2006) 094017, hep-ph/0604023.

[68] Jefferson Lab Hall B, . H.Avakian et al., LOI to PAC30 (2006).